

This article was downloaded by:

On: 16 January 2011

Access details: *Access Details: Free Access*

Publisher *Taylor & Francis*

Informa Ltd Registered in England and Wales Registered Number: 1072954 Registered office: Mortimer House, 37-41 Mortimer Street, London W1T 3JH, UK



Journal of Energetic Materials

Publication details, including instructions for authors and subscription information:

<http://www.informaworld.com/smpp/title~content=t713770432>

The initiation of small-diameter emulsion explosives by commercial detonators

David L. Kennedy^{abc}

^a Explosives Group Technical Centre Imperial Chemical Industries PLC Stevenston, Ayrshire, Scotland

^b Michael Kennedy and Ian D Kerr Explosion and Flame Laboratory Health and Safety Executive Harpur Hill, Buxton, Derbyshire, England ^c Research Group, ICI Australia Pty Ltd., Ascot Vale, Australia

To cite this Article Kennedy, David L.(1990) 'The initiation of small-diameter emulsion explosives by commercial detonators', *Journal of Energetic Materials*, 8: 1, 1 – 20

To link to this Article: DOI: 10.1080/07370659008017243

URL: <http://dx.doi.org/10.1080/07370659008017243>

PLEASE SCROLL DOWN FOR ARTICLE

Full terms and conditions of use: <http://www.informaworld.com/terms-and-conditions-of-access.pdf>

This article may be used for research, teaching and private study purposes. Any substantial or systematic reproduction, re-distribution, re-selling, loan or sub-licensing, systematic supply or distribution in any form to anyone is expressly forbidden.

The publisher does not give any warranty express or implied or make any representation that the contents will be complete or accurate or up to date. The accuracy of any instructions, formulae and drug doses should be independently verified with primary sources. The publisher shall not be liable for any loss, actions, claims, proceedings, demand or costs or damages whatsoever or howsoever caused arising directly or indirectly in connection with or arising out of the use of this material.

THE INITIATION OF SMALL-DIAMETER EMULSION EXPLOSIVES
BY COMMERCIAL DETONATORS

David L Kennedy*

Explosives Group Technical Centre
Imperial Chemical Industries PLC
Stevenston, Ayrshire KA20 3LN
Scotland

Michael Kennedy and Ian D Kerr
Explosion and Flame Laboratory
Health and Safety Executive
Harpur Hill, Buxton, Derbyshire SK17 9JN
England

ABSTRACT

Flash x-radiographs were obtained of commercial No 8* strength aluminium tube detonators in cartridges of emulsion explosive at various times after fusehead operation. The trigger system for the radiography was based on the detection of light following fusehead firing via optical fibres inserted into the fusehead cavity during detonator assembly. These experiments were simulated using a finite element hydrocode with realistic treatment of the non-ideal reaction kinetics. Excellent agreement between the simulation and experiment was demonstrated for the shape and position of the shock waves. Initiation of the emulsion explosive was predominately forward from the detonator, with the initiation in the reverse direction towards the crimped end of the detonator exhibiting both corner turning of the detonation front and dynamic desensitization.

* Present address : Research Group, ICI Australia Pty Ltd,
Newsom Street, Ascot Vale 3032, Australia

Journal of Energetic Materials vol. 8, 001-020 (1990)
Published in 1990 by Dowden, Brodman & Devine, Inc.

INTRODUCTION

In many of the commercial mining and quarrying operations carried out throughout the world, an essential prerequisite for safe and profitable blasting is the reliable initiation of a cartridge of explosive by a detonator.

However, relatively little is known about the phenomena controlling this initiation process. The amounts of explosive contained in these detonators are small, so that the detonation waves inside them will be highly time- and geometry- dependent, and thus cannot be described by simple models. The pressure from these detonations is then transmitted to the surroundings via the acceleration of the metal case, which itself will exhibit complex material response and failure. The buildup to detonation in the explosive cartridge is then further complicated by the interaction between the induced chemical reactions and the time-, geometry- and confinement- dependent hydrodynamic flow.

As a consequence of this complexity, although there has been a large body of experience accumulated on the initiation of different types of commercial explosive by different types of detonator, this information is largely anecdotal, and has resulted in little predictive or interpretative capability.

This paper will report on some of the results of a study aimed at elucidating the phenomena responsible for the buildup to initiation when typical commercial detonators interact with typical commercial explosives. The adopted approach combined flash X-radiography with detailed numerical simulation.

EXPERIMENTAL TECHNIQUE

Flash X-ray equipment was used to obtain radiographs of the early stages in the development of initiation and detonation in cartridges of emulsion explosive in the vicinity of the initiating detonator.

Explosive preparation

The explosive was an emulsion containing ammonium nitrate, water, oil and surfactant in the mass ratio 78.7:16.0:3.8:1.5, and

sensitized by the addition of sufficient glass-walled microspheres to lower the loading density to $\approx 1.05 \text{ g/cm}^3$. Control of void size was achieved by firstly sieving these microspheres and using only those with diameters in the range 75 - 90 μm , and secondly by removing under vacuum any air entrained during the mixing process.

The cartridges were each 100 mm long, and 27 mm diameter, preformed from thin waxed paper. This diameter was considerably larger than the experimental critical value of $\approx 7 \text{ mm}$ required to reliably transmit steady detonation in this emulsion.

The dependence of chemical reaction rate with pressure for this emulsion has been characterized by Leiper et al¹, and is representative of the class of emulsion compositions used in small-diameter applications (i.e. with cartridge diameters in the range $\approx 25 \text{ mm}$ to $\approx 75 \text{ mm}$).

Detonator preparation

The detonators, although especially assembled for this study, were intended to be notionally similar to the No 8* strength instantaneous electric type available commercially in the United Kingdom. This represents the highest strength detonator in common usage. Figure 1 presents a schematic diagram of the main features. The priming charge was $\approx 150 \text{ mg}$ of lead azide, with the base charge being $\approx 800 \text{ mg}$ pentaerythritol tetranitrate (PETN). This detonator was thus stronger than the minimum initiator of $\approx 150 \text{ mg}$ lead azide and $\approx 200 \text{ mg}$ PETN determined experimentally for the above emulsion.

The detonator cases were of aluminium, with flat end-caps. The dimensions of these tubes were : length $\approx 48 \text{ mm}$, external diameter $\approx 7.2 \text{ mm}$, wall thickness $\approx 0.4 \text{ mm}$.

A key modification was the incorporation during manufacture of a length of 2.25 mm diameter polymer-sheathed optical fibre into the fusehead cavity via the sealing plug.

Flash X-radiography

The X-ray equipment was a twin channel 300 kV Fexitron type 730/2710 system. Both channels produced a pulse of X-ray photons lasting $\approx 50 \text{ ns}$, being triggered by the experiment using two

independent delay circuits. The triggering event was the detection of light within the fusehead cavity of the detonator, transmitted to a remotely-situated fast-response photodetector and Schmitt trigger circuit by means of the optic fibre inserted into the detonator. All experiments were performed in an $\approx 80 \text{ m}^3$ steel chamber; Figure 2 shows schematically the experimental arrangement. Lead sheets were used to shield each film cassette from X-rays passing parallel to its face ; these have been omitted from Figure 2 for clarity.

The explosive cartridge was placed 2.3 m away from the X-ray tubes which were arranged to provide orthogonal views, and 180 mm from the faces of the film cassettes, giving rise to a total magnification of 1.1 for each image.

Event timing

During preliminary experiments, the output from both the photodetector and the Schmitt trigger circuit were monitored on a dual-channel transient recorder. Figure 3 shows voltage traces representing the extremes of observed behaviour. In each record, the trace with two small spikes in the plateau region is from the output of the Schmitt trigger, and the other trace is from the photodetector coupled to the optical fibre leading from the detonator. The X-ray tubes were fired at preset delay intervals in the range 0 to 15 μs after the step change in the Schmitt trigger output, giving rise to the spikes.

Figure 3a shows an abrupt change in the light level inside the fusehead cavity, with a risetime of $\approx 30 \text{ ns}$; the resulting radiographs had recorded a stage in the initiation event corresponding to the complete detonation of the detonator base charge.

On the other hand, Figure 3b shows a much longer risetime, of order 35 μs , for the light output, so that the X-ray tubes were fired before the light had reached its maximum. The images of the detonator obtained in this experiment were indistinguishable from that of an unfired detonator of the same type.

The cause of these two types of behaviour is not known. It is believed that, for the short risetime event, the position of the

optic fibre within the fusehead cavity together with its acceptance angle of 28° has excluded any light from the fusehead and from the initiation site of the lead azide, but has only accepted light generated as the detonation front has swept across the priming charge surface. The long risetime event would then arise when the acceptance angle allowed light to enter from both the fusehead and the priming charge.

Throughout the main body of experiments, the use of a high Schmitt trigger threshold voltage circumvented this variability in timing to some degree. Duplicate experiments using the same preset delay times indicated that the scatter in the relative trigger timing was thereby reduced to the order of 1 or 2 μs , but the absolute timing could not be determined.

NUMERICAL SIMULATION

The Lagrangian finite element hydrodynamic computer code DYNA2D, written by Hallquist², was used to simulate the experiments.

The computer representation of the pre-shot configuration is included in Figure 4 together with the corresponding radiograph. It has been necessary to simplify the simulation by omitting the fusehead; it was assumed that the primary charge was point initiated on the axis by the fusehead, and that onset of detonation in the lead azide was instantaneous. In preliminary simulations, the reaction rates for both the lead azide and PETN charges were described in detail by the Lee and Tarver Ignition and Growth model³, as modified by Kennedy⁴. However, a considerable saving in computational time was achieved by reverting to the simpler programmed burn option in DYNA2D², without compromising the degree of agreement with experiment to be discussed below.

The behaviour of the emulsion was simulated by a model specifically developed to provide a proper resolved reaction zone treatment of commercial explosives⁵. The reaction rate in this model is parameterized by fitting to experimental velocity of detonation versus cartridge diameter measurements (shown for this explosive by

Leiper et al¹) using the computer package CPEX which is based on a slightly divergent detonation theory for commercial explosives⁶.

A finite element mesh size of approximately 0.5 mm in the emulsion was found to be adequate to resolve the initiation process. The total number of elements in the simulations was then about 2000; each simulation required about 5 hours of CPU time on a MicroVAX II. Frequent use was made of the interactive rezoning facility in DYNA2D to enable the Lagrangian finite element mesh to follow the gross distortion occurring at the azide/PETN/detonator case conjunction point, after first establishing that the results of the simulations were not sensitive to slight variations in the details of the rezoning process. Even with the rezoner, the simulation could only be followed to 6.5 μ s prior to mesh collapse.

INTERPRETATION OF RESULTS

Only the results for one particular type of detonator, namely of No.8* strength and with a flat end-cap aluminium case, will be presented here, though the interpretation and discussion is based on observations made with other detonator types. Nine such detonators were radiographed, so that the double X-ray tube arrangement of Figure 2 provided eighteen views or stages covering the detonation within the detonator and the subsequent initiation of the emulsion.

Figure 4 presents a radiograph of an unfired detonator in an emulsion cartridge, together with the computer representation on the same scale. It can be seen that the fusehead is not lying axially within the detonator, due to the insertion of the optic fibre (which itself cannot be seen due to its low X-ray absorption) into a fuse-head cavity that was not initially designed to allow room for it.

Figure 5, presenting selected radiographs, and Figures 6 to 8, summarizing the computer simulation, should be viewed together.

In view of the uncertainties and the scatter in the triggering times as described previously, any time ascribed to a radiograph is nominal. The times quoted in Figure 5 have been assigned after a detailed comparison with the simulation, where the time elapsed since initiation of the primary charge is known accurately.

Since X-ray attenuation through a material is proportional to its density, Figure 6, showing the predicted density field, may be compared with the experimental radiographs of Figure 5. Apart from some asymmetries in the radiographs, the experiment and the simulation are seen to be in remarkable agreement on all the significant observable features.

Analysis at 2.0 μ s

The detonation front in the PETN is observable roughly two-thirds of the way along the base charge. The aluminium case is expanding, driving a shock wave into the surrounding explosive.

Analysis at 3.0 μ s

The detonation front in the PETN has consumed all of that explosive, and has encountered the end-cap, which because of its higher shock impedance, has reflected a shock wave backwards through the PETN detonation products. The simulations indicate that the highest pressure delivered by this type of detonator to the surrounding explosive is located immediately above the end-cap, and that the rim of this type of flat end-cap interferes with the transfer of pressure into the surrounding explosive. It is helpful to consider the shock waves emerging (spherically) from the end-cap and (cylindrically) from the sides of the detonator as being distinct at this early stage of the initiation process. This two wave structure is visible in the radiograph of Figure 5, though it was more apparent in radiographs of other types of detonators, for which space does not permit inclusion in this paper.

It can be seen that the reverse wave (i.e., the wave directed downwards as the figures are viewed, towards the crimped end of the detonator) has propagated over a much shorter distance than has the wave propagating radially outwards. A lower shock velocity implies that the shock wave is being driven by a lower pressure ; this is confirmed by Figure 7, which indicates that the pressure in the emulsion surrounding the fusehead cavity is less than 1 GPa, whereas the pressure in the shock propagating radially outwards is of order 4 - 5 GPa. This radial shock wave is in fact accelerating due to the

energy being fed into it by the induced chemical reaction - Figure 8 indicates that the degree of chemical reaction (or equivalently the release of the available chemical energy in the emulsion) is over 90% completed in the emulsion enveloped by this wave.

Analysis at 4.5 μ s

By 4.5 μ s, the radial shock wave has encountered the cartridge outer boundary, and material is being rapidly ejected outwards. The resulting rarefaction wave is lowering the pressure, and quenching further chemical reaction there.

A clear distinction has become apparent between the initiation process in the forward direction (that is, upwards from the end-cap as the figures are viewed) as compared to the reverse direction.

In the forward direction, the front of the wave has become much smoother than that shown at 3.0 μ s, though it is still strongly curved close to the axis of the cartridge. The simulation, shown in Figure 7 (though more apparent in full colour than in the present grey-scale version), indicates that the highest pressure is no longer above the end-cap at the axis of the cartridge, but is out towards the edges of the cartridge, on the shock wave that expanded radially from the sides of the detonator. This is a consequence of the initial two-wave structure mentioned above for 3.0 μ s. The shock wave emerging from the end-cap is roughly spherical in shape, and thus has a higher divergence than the shock emerging from the sides of the detonator which is roughly cylindrical in shape. In an inert material, this extra divergence would result in the wave from the end-cap attenuating at a faster rate than the wave from the sides. In the reactive emulsion, the flow is more complex, but the same basic argument still applies.

Since the chemical reaction rate increases with increasing shock pressure, it can be seen from Figure 8 that this region of highest pressure towards the edges of the cartridge is associated with the fastest reaction rates.

It should be noted in Figure 7 that the pressure remaining inside the head of the detonator in the PETN product gases has

dropped below the pressure in the surrounding reacting emulsion. Close inspection of the radiographs has confirmed that the aluminium case in this region reaches its maximum expansion at about $4.0 \mu\text{s}$, and subsequently begins to collapse back towards the axis.

In the reverse direction, the experimental radiograph is indicating asymmetrical behaviour, with the reverse wave on the right hand side being slightly retarded when compared to the left hand side. It is significant that the fusehead is not central within the detonator, but is lying closer to the right hand side. It is postulated that the heat generated by the pyrotechnic reaction of the fusehead has both preferentially weakened the aluminium case and has initiated the lead azide priming charge on that side. This combination has led to the tube rupturing first in that region, allowing the surrounding emulsion explosive to flow into the fuse-head cavity (in light of the pressure gradient mentioned above) with the resulting local drop in pressure acting to quench reaction and to slow down the wave propagation.

Analysis at $6.5 \mu\text{s}$

The radius of curvature of the front in the forward direction has increased, and is close in value to that of the final steady-state detonation front. The low pressure region on the axis has almost been enveloped by the adjacent high pressure regions ; by $7 \mu\text{s}$, this will have been completed. The shape of the isobars behind the front will continue to evolve at a slow rate over several more microseconds until steady state is reached. Separate experiments on longer length charges confirmed that steady detonation was indeed always achieved with this combination of detonator and emulsion.

The effect of no confinement is seen in the quenching of reaction at the sides of the cartridge in Figure 8.

Both the radiograph and the density field are showing that a two-wave structure has developed in the reverse direction in the region of the fusehead. Its origin is believed to be as follows. As noted previously, only a low pressure shock is initially sent into this region. This low pressure collapses the glass microspheres in

the emulsion with insufficient violence to create hotspots with the intensity required to initiate and sustain an outward burning flame front. As Figure 8 shows, the induced extent of chemical reaction therefore remains low, and insufficient energy is released to accelerate this initial shock into a detonation wave. The pressure in the explosive here is further decreased as the detonator tube collapses inwards into the free space of the fusehead cavity. This initial shock has, however, removed the voidage in, and thus has desensitized⁷, the emulsion explosive around the fusehead cavity. On the other hand, the pressure sent forward from the detonator was of sufficient intensity to cause self-acceleration. This high pressure is now corner turning and spreading down towards the explosive surrounding the fusehead region, and is visible as the second compressive wave. Where it encounters desensitized explosive close to the detonator, it cannot create further hotspot activity, so that the induced reaction rate remains low. However, with its faster wave velocity, it has overtaken the initial low pressure wave close to the cartridge boundary, and, since it is propagating through undisturbed explosive, is able to self-accelerate up to detonation.

It is thus seen that, in the reverse direction, initiation and buildup to detonation occurs in an annulus away from the detonator tube and close to the cartridge boundary. It is also apparent that if the diameter of the cartridge were to be reduced slightly, there would be no path available for the initiating shock to propagate down past the fusehead region of the detonator. In this case, that part of the emulsion explosive surrounding the crimped end of the detonator would probably be recovered intact after the shot had been fired.

DISCUSSION

It has been established that, at least with the present combination of detonator and explosive, the initiation process was strongly directional, with build-up to detonation occurring primarily in the forward direction. Indeed, detonation was not induced directly in the reverse direction, but rather was a

consequence of that forward initiation.

This has several important implications for the use of small-diameter explosive cartridges in typical mining applications.

Firstly, reverse initiation from a detonator will be far more dependent upon cartridge diameter than will forward initiation. This was verified by a separate experiment at this laboratory, where forward initiation of this emulsion explosive by a No 8* strength detonator was found to occur for cartridge diameters greater than 7 mm, whereas reverse initiation was ensured only in cartridge diameters exceeding 15 mm. When the emulsion density was increased to 1.20 g/cm^3 by reducing the volume fraction of microspheres, the critical diameter for forward initiation increased to be 15 mm, while that for reverse initiation increased to be over 35 mm.

Secondly, reverse initiation will be less dependent upon detonator strength (i.e. the mass of the PETN base charge) than will forward initiation. As the strength of the detonator increases, the duration of the pressure pulse induced in the reverse direction increases, but its intensity does not. Hence, desensitization will still occur in the emulsion surrounding the fusehead cavity region. The reverse wave will decay more slowly, travel faster, and thus desensitize more explosive for increased detonator strength. However, counterbalancing this, forward initiation will occur more quickly. In a confirmatory experiment, it was found that a No 6 strength detonator (with a base charge of $\approx 250 \text{ mg}$ PETN) required the same minimum cartridge diameter for reverse initiation as did the No 8* detonator.

It is thus apparent that if misfires are to be avoided in mines, it is important that minimum initiator and critical diameter tests on small-diameter explosive products should investigate initiation in both the forward and the reverse direction from the detonator.

ACKNOWLEDGEMENTS

The authors would like to acknowledge the work done by Miss Ann Steele in assembling the detonators and preparing the emulsion

explosive. John Geller suggested the use of the optic fibre triggering system. The permission of the ICI companies worldwide and the Health and Safety Executive to publish this paper is gratefully acknowledged.

REFERENCES

1. G A Leiper, I J Kirby and A Hackett, Eighth Symposium (International) on Detonation, 1985, (Naval Surface Weapons Center, Maryland, NSWC MP 86-194, 1986), p.187.
2. J O Hallquist, "User's Manual for DYNA2D - An Explicit Two-Dimensional Hydrodynamic Finite Element Code with Interactive Rezoning", Lawrence Livermore Laboratory report UCID-18756, Rev. 3, March 1988.
3. E L Lee and C M Tarver, Phys. Fluids 23 2362 (1980).
4. D L Kennedy, Fourth MoD(PE) Detonics Working Group Seminar, Cambridge, England, March 14th, 1986
5. D L Kennedy, DYNA3D User Group Conference, London, England, September 24th, 1987.
6. I J Kirby and G A Leiper, Eighth Symposium (International) on Detonation, 1985, (Naval Surface Weapons Center, Maryland, NSWC MP 86-194, 1986), p.176.
7. A W Campbell, W C Davis, J B Ramsay and J R Travis, Phys. Fluids 4 511 (1961).

British Crown Copyright 1988.

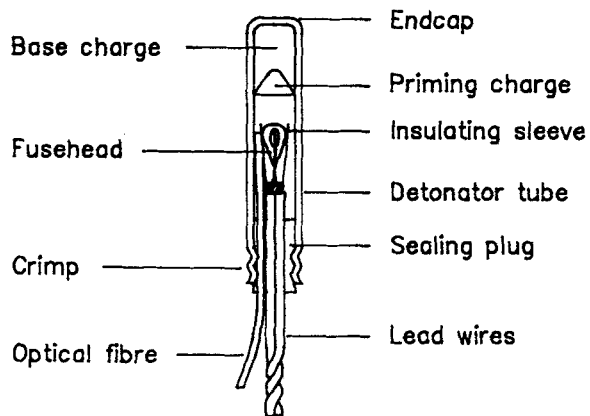


FIGURE 1.

Schematic representation of a No 8* instantaneous electric aluminium tube detonator, as modified to include an optic fibre.

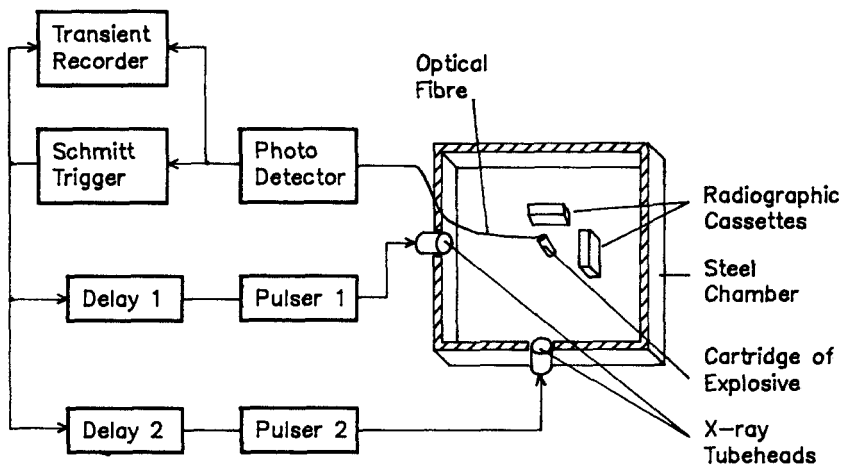


FIGURE 2.

Schematic representation of experimental arrangement.

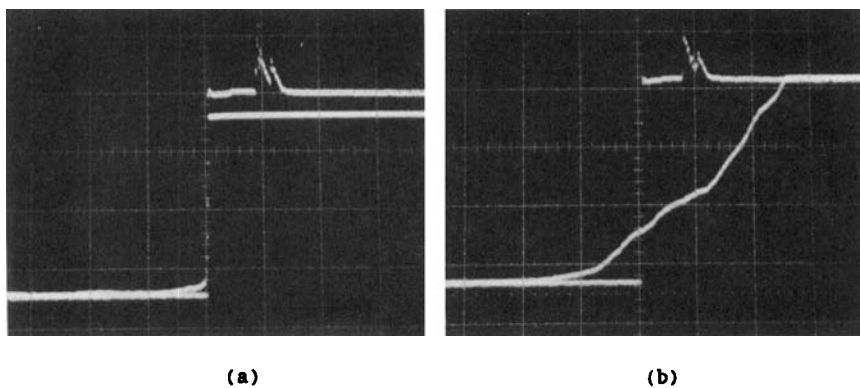


FIGURE 3.

Representative transient recorder traces of the photodetector output and the Schmitt-trigger circuit output (with the two spikes) showing extremes of (a) short and (b) long risetimes for the light detection within the fusehead cavity. The horizontal scale is 10 μ s per centimetre division; the vertical scale is 1 V per centimetre division.

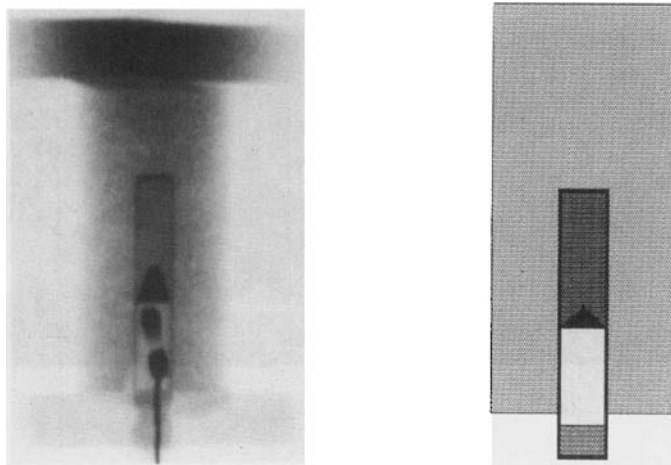
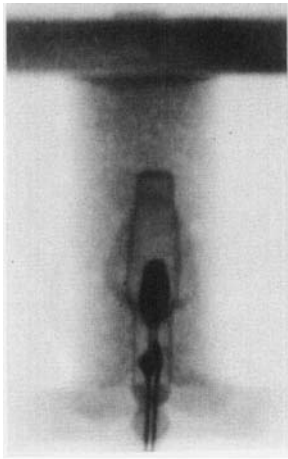
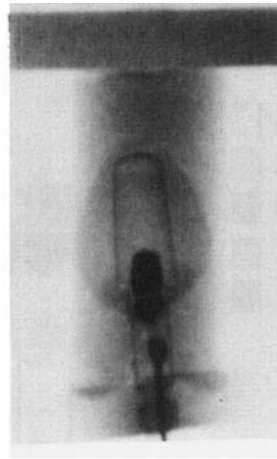


FIGURE 4.

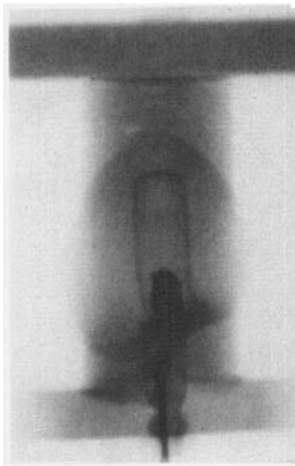
Computer-enhanced X-radiograph and corresponding finite element representation of the preshot configuration of a detonator in a 27 mm diameter cartridge of emulsion explosive. The optic fibre provides insufficient X-ray absorption to be visible.



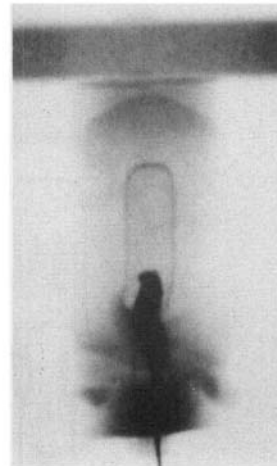
2.0 μ s



3.0 μ s



4.5 μ s



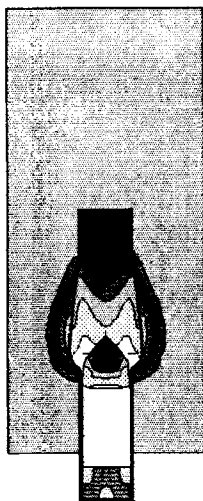
6.5 μ s

FIGURE 5.

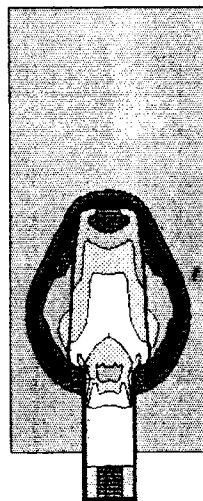
Computer-enhanced flash X-radiographs of various stages of the initiation of the emulsion explosive by the detonator. The times are nominal, and are relative to the initiation of the lead azide primary charge.

g/cm^3

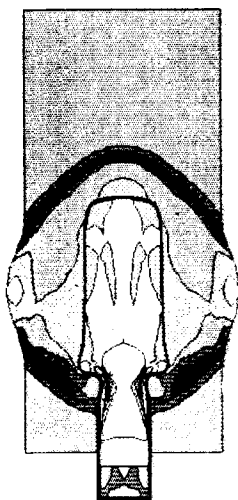
0.55	□
0.83	▨
1.10	■
1.37	■
1.65	■



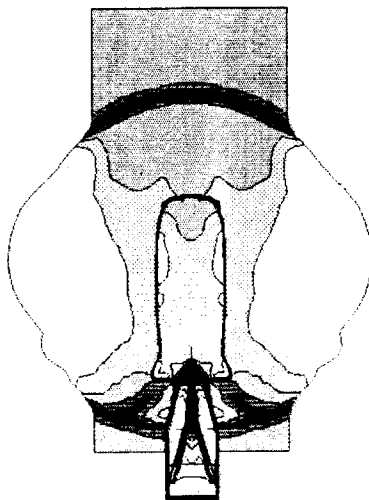
2.0 μsec



3.0 μsec



4.5 μsec



6.5 μsec

FIGURE 6.

Predicted density field from the finite element simulation at various times after initiation of the lead azide primary charge.

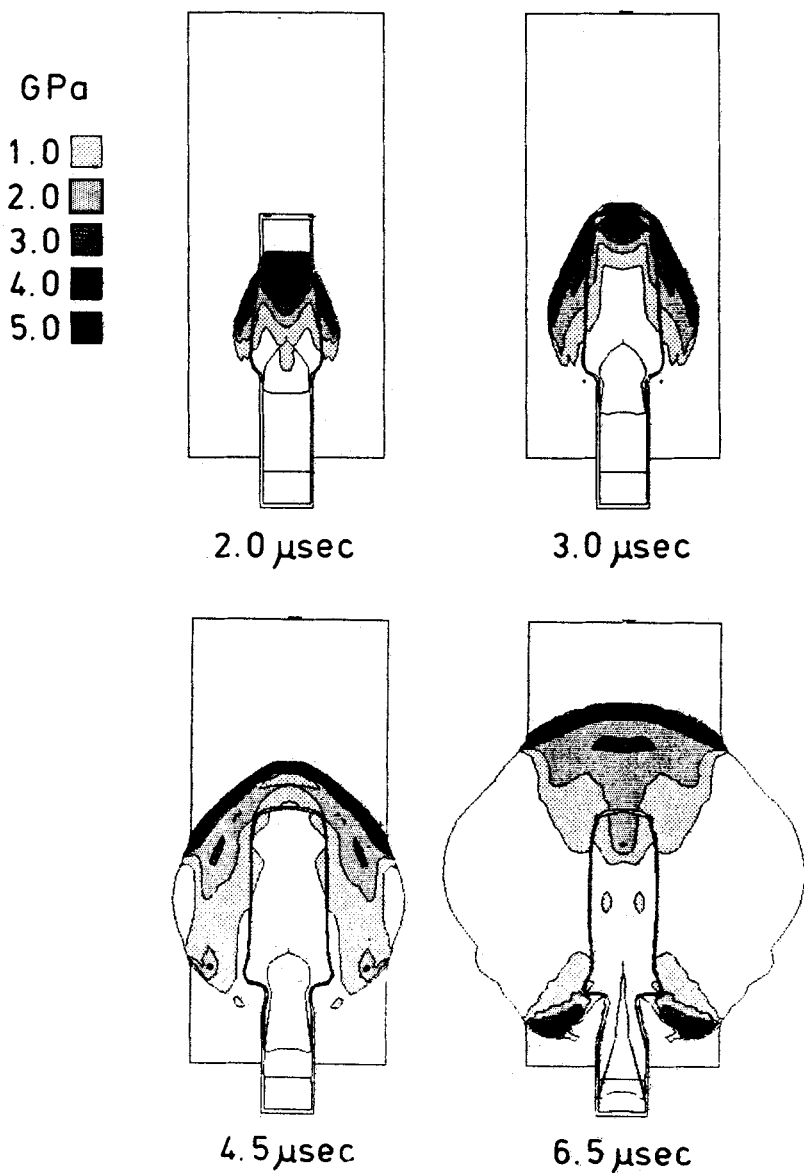


FIGURE 7.

Predicted pressure field from the finite element simulation at various times after initiation of the lead azide primary charge.

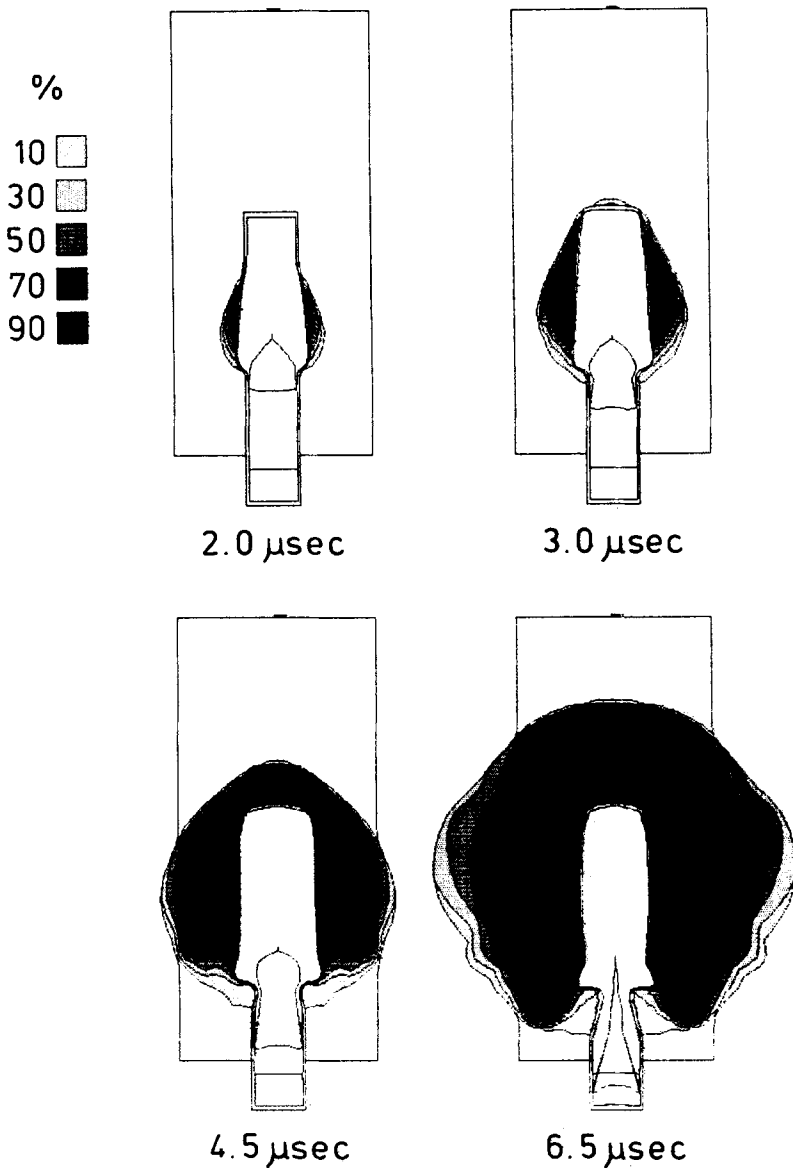


FIGURE 8.

Predicted extent of reaction field for the emulsion explosive from the finite element simulation at various times after initiation of the lead azide primary charge.